AIP | The Journal of Chemical Physics

A highly accurate ab initio potential energy surface for methane

Alec Owens, Sergei N. Yurchenko, Andrey Yachmenev, Jonathan Tennyson, and Walter Thiel

Citation: The Journal of Chemical Physics **145**, 104305 (2016); doi: 10.1063/1.4962261
View online: http://dx.doi.org/10.1063/1.4962261
View Table of Contents: http://scitation.aip.org/content/aip/journal/jcp/145/10?ver=pdfcov
Published by the AIP Publishing

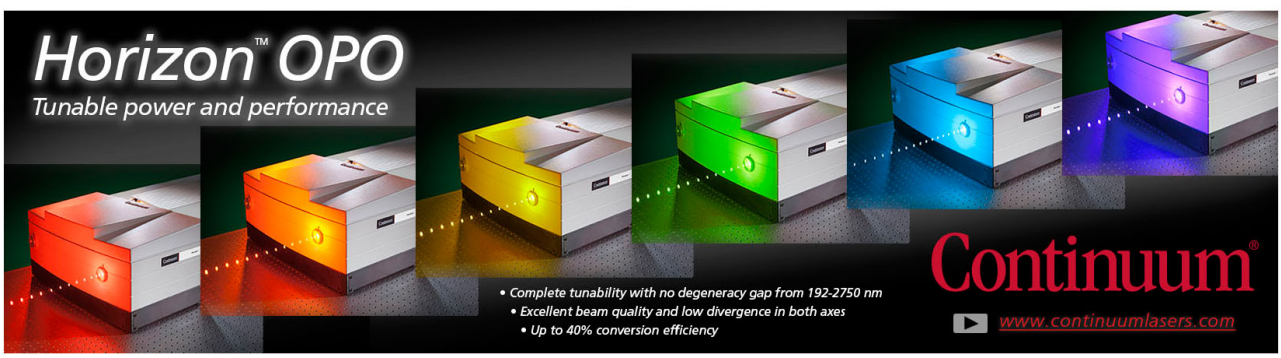

A highly accurate *ab initio* potential energy surface for methane

Alec Owens,[1,2,a)] Sergei N. Yurchenko,[1] Andrey Yachmenev,[1] Jonathan Tennyson,[1] and Walter Thiel[2]
[1]*Department of Physics and Astronomy, University College London, Gower Street, WC1E 6BT London, United Kingdom*
[2]*Max-Planck-Institut für Kohlenforschung, Kaiser-Wilhelm-Platz 1, 45470 Mülheim an der Ruhr, Germany*

(Received 24 June 2016; accepted 24 August 2016; published online 9 September 2016)

A new nine-dimensional potential energy surface (PES) for methane has been generated using state-of-the-art *ab initio* theory. The PES is based on explicitly correlated coupled cluster calculations with extrapolation to the complete basis set limit and incorporates a range of higher-level additive energy corrections. These include core-valence electron correlation, higher-order coupled cluster terms beyond perturbative triples, scalar relativistic effects, and the diagonal Born-Oppenheimer correction. Sub-wavenumber accuracy is achieved for the majority of experimentally known vibrational energy levels with the four fundamentals of $^{12}CH_4$ reproduced with a root-mean-square error of 0.70 cm^{-1}. The computed *ab initio* equilibrium C–H bond length is in excellent agreement with previous values despite pure rotational energies displaying minor systematic errors as J (rotational excitation) increases. It is shown that these errors can be significantly reduced by adjusting the equilibrium geometry. The PES represents the most accurate *ab initio* surface to date and will serve as a good starting point for empirical refinement. *Published by AIP Publishing.* [http://dx.doi.org/10.1063/1.4962261]

I. INTRODUCTION

As a key atmospheric molecule the infrared spectrum of methane (CH_4) has been the subject of numerous studies. Its complex polyad structure is beginning to be explored in greater detail at higher energies,[1–26] and there is strong motivation to continue working towards the visible region to aid the study of exoplanets.[27] Variational calculations from first principles were recently used in conjunction with an experimental line list[28] to assign a significant number of vibrational band centers in the icosad range (6300–7900 cm^{-1}).[25] This kind of analysis could prove extremely useful for more congested regions and its success depends on having a reliable potential energy surface (PES) to work with.

The construction of highly accurate PESs for small polyatomic molecules has seen remarkable progress in recent years. It is now possible to compute vibrational energy levels within "spectroscopic accuracy" (better than ±1 cm^{-1}) using a purely *ab initio* PES.[29–34] To do so requires the use of a one-particle basis set near the complete basis set (CBS) limit, and the consideration of additional, higher-level (HL) contributions to recover more of the electron correlation energy.[35,36] Although computationally demanding, these can be routinely calculated with most quantum chemistry codes.

A number of accurate PESs for CH_4 have been reported in the literature.[30,37–48] These include purely *ab initio* surfaces,[30,37,41–43,48] and those which are based on *ab initio* calculations but have subsequently been refined to experiment.[38–40,44–47] The most rigorous *ab initio* treatment to date was by Schwenke[30] who accounted for several HL contributions. Corrections to the full configuration interaction (CI) limit, core-valence (CV) electron correlation, scalar relativistic (SR) effects, the Lamb shift, the diagonal Born-Oppenheimer correction (DBOC), non-adiabatic corrections, as well as extrapolation of the basis set to the CBS limit were all treated at some level. Whilst low-lying states of $^{12}CH_4$ were reproduced with sub-wavenumber accuracy, the description of the stretching fundamentals, ν_1 and ν_3, was relatively poor in comparison and the errors in vibrational energies gradually increased after 3000 cm^{-1}.

As part of the ExoMol project,[49,50] a comprehensive methane line list, 10to10,[46] was produced by two of the authors. This line list represented a significant step forward in the variational treatment of five-atom molecules, and 10to10 has facilitated the detection of CH_4 in brown dwarfs,[46] T dwarfs,[51] and the hot Jupiter exoplanet HD 189733b.[52] Since its construction a number of high resolution spectroscopic measurements on methane above the tetradecad region (above 6300 cm^{-1}) have been reported.[20–25] There have also been key developments[53] in our nuclear motion code TROVE[54] which considerably improves basis set convergence; a major bottleneck in the past. Given the demand for comprehensive methane data at higher energies and the knowledge we have acquired from the 10to10 line list, it seems natural to begin working on a more extensive and accurate treatment of CH_4.

In this work we present a state-of-the-art *ab initio* PES for methane. After fitting the *ab initio* data with a symmetrized analytic representation, the PES is evaluated with variational calculations of pure rotational and $J = 0$ energy levels. To ensure a reliable assessment, fully converged vibrational term values are obtained by means of a complete vibrational basis set (CVBS) extrapolation.[55]

The paper is structured as follows: In Sec. II the electronic structure calculations and analytic representation of the PES

a)Electronic mail: alec.owens.13@ucl.ac.uk

are presented. The variational nuclear motion computations used to validate the PES are described in Sec III. In Sec. IV, vibrational $J = 0$ energy levels for $^{12}CH_4$, the equilibrium C–H bond length, and pure rotational energies up to $J = 10$ are calculated and compared with available experimental results. We offer concluding remarks in Sec. V.

II. POTENTIAL ENERGY SURFACE

A. Electronic structure calculations

The approach employed for the electronic structure calculations is almost identical to our previous work on SiH_4.[34] The aim is to generate a PES which has the "correct" shape and computing tightly converged energies with respect to basis set size for the HL corrections is not as important. The levels of theory and basis sets have therefore been chosen to strike a balance between accuracy and computational cost.

Utilizing focal-point analysis[56] the total electronic energy is written as

$$E_{\text{tot}} = E_{\text{CBS}} + \Delta E_{\text{CV}} + \Delta E_{\text{HO}} + \Delta E_{\text{SR}} + \Delta E_{\text{DBOC}}. \quad (1)$$

The energy at the complete basis set (CBS) limit E_{CBS} was computed using the explicitly correlated F12 coupled cluster method CCSD(T)-F12b (Ref. 57) in conjunction with the F12-optimized correlation consistent polarized valence basis sets, cc-pVTZ-F12 and cc-pVQZ-F12.[58] The frozen core approximation was employed and calculations used the diagonal fixed amplitude ansatz 3C(FIX)[59] with a Slater geminal exponent value of $\beta = 1.0\, a_0^{-1}$.[60] For the auxiliary basis sets (ABS), the OptRI,[61] cc-pV5Z/JKFIT,[62] and aug-cc-pwCV5Z/MP2FIT[63] were used for the resolution of the identity (RI) basis and the two density fitting (DF) basis sets, respectively. Calculations were carried out with MOLPRO2012[64] unless stated otherwise.

To extrapolate to the CBS limit we used the parameterized, two-point formula[60]

$$E^C_{\text{CBS}} = (E_{n+1} - E_n)F^C_{n+1} + E_n. \quad (2)$$

The coefficients F^C_{n+1}, which are specific to the CCSD-F12b and (T) components of the total CCSD(T)-F12b energy, had values of $F^{\text{CCSD-F12b}} = 1.363\,388$ and $F^{(\text{T})} = 1.769\,474$.[60] No extrapolation was applied to the Hartree-Fock (HF) energy, rather the HF+CABS (complementary auxiliary basis set) singles correction[57] calculated in the larger basis set was used.

The contribution from core-valence (CV) electron correlation ΔE_{CV} was computed at the CCSD(T)-F12b level of theory with the F12-optimized correlation consistent core-valence basis set cc-pCVTZ-F12.[65] Calculations employed the same ansatz and ABS as used for E_{CBS}, however, the Slater geminal exponent was changed to $\beta = 1.4\, a_0^{-1}$.

Higher-order (HO) correlation effects were accounted for using the hierarchy of coupled cluster methods such that $\Delta E_{\text{HO}} = \Delta E_{\text{T}} + \Delta E_{(\text{Q})}$. Here, the full triples contribution is $\Delta E_{\text{T}} = \left[E_{\text{CCSDT}} - E_{\text{CCSD(T)}}\right]$, and the perturbative quadruples contribution is $\Delta E_{(\text{Q})} = \left[E_{\text{CCSDT(Q)}} - E_{\text{CCSDT}}\right]$. Calculations were performed in the frozen core approximation at the CCSD(T), CCSDT, and CCSDT(Q) levels of theory using the general coupled cluster approach[66,67] as implemented in the MRCC code[68] interfaced to CFOUR.[69] The correlation consistent triple zeta basis set, cc-pVTZ,[70] was utilized for the full triples contribution, whilst the perturbative quadruples employed the double zeta basis set, cc-pVDZ.

The scalar relativistic (SR) correction ΔE_{SR} was calculated with the second-order Douglas-Kroll-Hess approach[71,72] at the CCSD(T)/cc-pVQZ-DK[73] level of theory in the frozen core approximation. For light, closed-shell molecules the spin-orbit interaction can be neglected in spectroscopic calculations.[74]

The diagonal Born-Oppenheimer correction (DBOC) ΔE_{DBOC} was computed with all electrons correlated using the CCSD method[75] as implemented in CFOUR with the aug-cc-pCVDZ basis set. The DBOC has a noticeable effect on vibrational term values of methane[30] but because it is mass dependent its inclusion means that the PES is only applicable for $^{12}CH_4$.

All terms in Eq. (1) were calculated on a grid of 97 721 geometries with energies up to $hc \cdot 50\,000$ cm^{-1} (h is the Planck constant and c is the speed of light). The global grid was built in terms of nine internal coordinates; four C–H bond lengths r_1, r_2, r_3, and r_4, and five $\angle(\text{H}_j\text{–C–H}_k)$ interbond angles α_{12}, α_{13}, α_{14}, α_{23}, and α_{24}, where j and k label the respective hydrogen atoms. The C–H stretch distances ranged from $0.71 \le r_i \le 2.60$ Å for $i = 1,2,3,4$ whilst bending angles varied from $40° \le \alpha_{jk} \le 140°$, where $jk = 12,13,14,23,24$.

Although it is computationally demanding to calculate the HL corrections at every grid point, it is actually time-effective given the system size, levels of theory, and basis sets used. Timing data are shown in Table I and we see that it takes just over 15 min to compute all the contributions in Eq. (1) at the equilibrium geometry. Naturally this time will increase as we stretch and bend the molecule due to slower energy convergence, with calculations needing at most 2–3 times longer for highly distorted geometries.

Alternatively, one can compute each HL correction on a reduced grid, fit a suitable analytic representation to the data, and then interpolate to other points on the global grid (see Refs. 31 and 33 for examples of this strategy). For more demanding systems this approach can significantly reduce computational time, however, obtaining an adequate description of each HL correction requires careful consideration and may not be straightforward. These issues are avoided in our present approach.

TABLE I. Wall clock times (seconds) for the different contributions to the potential energy surface. Calculations were performed on a single core of an Intel Xeon E5-2690 v2 3.0 GHz processor. Timings shown have been averaged over 10 runs for one point at the equilibrium geometry.

Contribution	No. of calculations required per point	Time
E_{CBS}	2	296
ΔE_{CV}	2	107
ΔE_{HO}	3	234
ΔE_{SR}	2	189
ΔE_{DBOC}	1	87
E_{tot}	10	913

B. Analytic representation

The XY_4 symmetrized analytic representation employed for the present study has previously been used for methane[45,46] and silane.[34] Morse oscillator functions describe the stretch coordinates,

$$\xi_i = 1 - \exp\left(-a(r_i - r_{\text{ref}})\right),\ i = 1,2,3,4, \tag{3}$$

where $a = 1.845\ \text{Å}^{-1}$ and the reference equilibrium structural parameter $r_{\text{ref}} = 1.085\,94$ Å (value discussed in Sec. IV B). For the angular terms we use symmetrized combinations of interbond angles,

$$\xi_5 = \frac{1}{\sqrt{12}}\left(2\alpha_{12} - \alpha_{13} - \alpha_{14} - \alpha_{23} - \alpha_{24} + 2\alpha_{34}\right), \tag{4}$$

$$\xi_6 = \frac{1}{2}\left(\alpha_{13} - \alpha_{14} - \alpha_{23} + \alpha_{24}\right), \tag{5}$$

$$\xi_7 = \frac{1}{\sqrt{2}}\left(\alpha_{24} - \alpha_{13}\right), \tag{6}$$

$$\xi_8 = \frac{1}{\sqrt{2}}\left(\alpha_{23} - \alpha_{14}\right), \tag{7}$$

$$\xi_9 = \frac{1}{\sqrt{2}}\left(\alpha_{34} - \alpha_{12}\right). \tag{8}$$

The potential function,

$$V(\xi_1,\xi_2,\xi_3,\xi_4,\xi_5,\xi_6,\xi_7,\xi_8,\xi_9) = \sum_{ijk\ldots} \mathrm{f}_{ijk\ldots} V_{ijk\ldots}, \tag{9}$$

which has maximum expansion order $i + j + k + l + m + n + p + q + r = 6$, is composed of the terms

$$V_{ijk\ldots} = \{\xi_1^i \xi_2^j \xi_3^k \xi_4^l \xi_5^m \xi_6^n \xi_7^p \xi_8^q \xi_9^r\}^{T_{\text{d}}(\text{M})}, \tag{10}$$

where $V_{ijk\ldots}$ are symmetrized combinations of different permutations of the coordinates ξ_i and transform according to the A_1 representation of the T_{d}(M) molecular symmetry group.[76] The terms in Eq. (10) are found by solving an over-determined system of linear equations in terms of the nine coordinates given above. In total there are 287 symmetrically unique terms up to sixth order, of which only 110 were employed for the final PES.

A least-squares fitting to the *ab initio* data was used to determine the expansion parameters $\mathrm{f}_{ijk\ldots}$. Weight factors of the form suggested by Partridge and Schwenke[77]

$$w_i = \left(\frac{\tanh\left[-0.0006 \times (\tilde{E}_i - 15\,000)\right] + 1.002\,002\,002}{2.002\,002\,002}\right) \times \frac{1}{N\tilde{E}_i^{(w)}} \tag{11}$$

were utilized in the fit. Here, $\tilde{E}_i^{(w)} = \max(\tilde{E}_i, 10\,000)$, where $\tilde{E}_i$ is the potential energy at the ith geometry above equilibrium and the normalization constant $N = 0.0001$ (all values in cm^{-1}). In our fitting, energies below 15 000 cm^{-1} are favoured by the weighting scheme. To further improve the description at lower energies and reduce the weights of outliers, we employed Watson's robust fitting scheme.[78] The final PES was fitted with a weighted root-mean-square (rms) error of 1.08 cm^{-1} for energies up to $hc \cdot 50\,000$ cm^{-1} and required 112 expansion parameters ($110 + r_{\text{ref}} + a$).

For geometries where $r_i \geq 1.80$ Å for $i = 1,2,3,4$, the respective weights were dropped by several orders of magnitude. At larger stretch distances a T1 diagnostic value >0.02 indicates that the coupled cluster method has become unreliable.[79] Energies are not wholly accurate at these points but they are still useful; their inclusion ensures that the PES maintains a reasonable shape towards dissociation. In subsequent calculations we refer to this PES as CBS-F12$^{\text{HL}}$. The CBS-F12$^{\text{HL}}$ expansion parameter set is provided in the supplementary material along with a FORTRAN routine to construct the PES.

III. VARIATIONAL CALCULATIONS

The general methodology of TROVE is well documented[53,54,80] and calculations on methane have previously been reported.[45,46] We therefore summarize only the key aspects relevant for this work.

The rovibrational Hamiltonian was represented as a power series expansion around the equilibrium geometry in terms of the nine coordinates introduced in Eqs. (3)–(8). However, for the kinetic energy operator linear displacement variables $(r_i - r_{\text{ref}})$ were used for the stretching coordinates. The Hamiltonian was constructed numerically using an automatic differentiation method[53] with the kinetic and potential energy operators truncated at 6th and 8th order, respectively. A discussion of the associated errors of such a scheme can be found in Refs. 53 and 54. Atomic mass values were used throughout.

A multi-step contraction scheme was employed to construct the vibrational basis set, the size of which is controlled by the polyad number,

$$P = 2(n_1 + n_2 + n_3 + n_4) + n_5 + n_6 + n_7 + n_8 + n_9 \leq P_{\max}, \tag{12}$$

and this does not exceed a predefined maximum value $P_{\max}$. As shown in Fig. 1, the size of the Hamiltonian matrix grows exponentially with respect to $P_{\max}$ and calculations above $P_{\max} = 14$ have not been possible with the resources available to us. Here the quantum numbers n_k for $k = 1,\ldots,9$

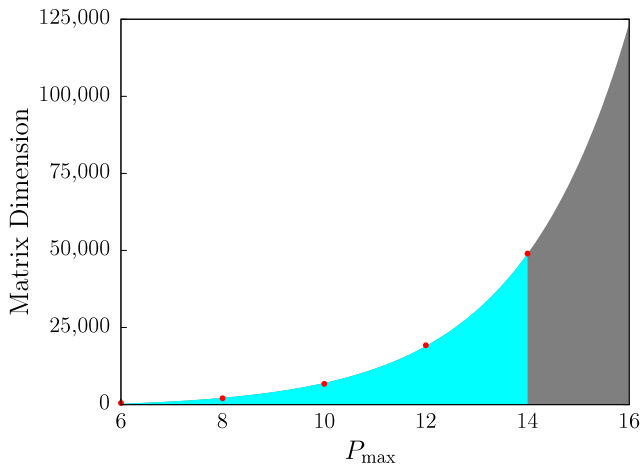

FIG. 1. Size of the $J = 0$ Hamiltonian matrix with respect to the polyad truncation number $P_{\max}$. Calculations have not been possible above $P_{\max} = 14$.

TABLE II. Comparison of calculated and experimental $J = 0$ vibrational term values (in cm^{-1}) up to the tetradecad region for $^{12}CH_4$. The zero-point energy was computed to be 9708.846 cm^{-1} at the CVBS limit.

Mode	Sym.	Experiment	Calculated	Obs–calc	Reference
ν_4^1	F_2	1310.76	1310.24	0.52	5
ν_2^1	E	1533.33	1533.04	0.29	5
$2\nu_4^0$	A_1	2587.04	2585.74	1.30	5
$2\nu_4^2$	F_2	2614.26	2613.04	1.22	5
$2\nu_4^2$	E	2624.62	2624.08	0.54	5
$\nu_2^1+\nu_4^1$	F_2	2830.32	2829.71	0.61	5
$\nu_2^1+\nu_4^1$	F_1	2846.07	2845.44	0.63	5
ν_1	A_1	2916.48	2917.16	−0.68	5
ν_3^1	F_2	3019.49	3020.57	−1.08	5
$2\nu_2^0$	A_1	3063.65	3063.04	0.61	5
$2\nu_2^2$	E	3065.14	3064.53	0.61	5
$3\nu_4^1$	F_2	3870.49	3869.18	1.31	5
$3\nu_4^1$	A_1	3909.20	3907.11	2.09	5
$3\nu_4^3$	F_1	3920.50	3919.01	1.49	18
$3\nu_4^3$	F_2	3930.92	3930.00	0.92	5
$\nu_2^1+2\nu_4^0$	E	4101.39	4100.52	0.87	5
$\nu_2^1+2\nu_4^2$	F_1	4128.77	4127.77	1.00	18
$\nu_2^1+2\nu_4^2$	A_1	4132.88	4132.21	0.67	18
$\nu_2^1+2\nu_4^2$	F_2	4142.86	4142.03	0.83	18
$\nu_2^1+2\nu_4^2$	E	4151.20	4150.62	0.58	18
$\nu_2^1+2\nu_4^2$	A_2	4161.84	4161.00	0.84	18
$\nu_1+\nu_4^1$	F_2	4223.46	4223.62	−0.16	5
$\nu_3^1+\nu_4^1$	F_2	4319.21	4319.37	−0.16	5
$\nu_3^1+\nu_4^1$	E	4322.18	4323.38	−1.20	5
$\nu_3^1+\nu_4^1$	F_1	4322.58	4323.53	−0.95	18
$\nu_3^1+\nu_4^1$	A_1	4322.72	4323.01	−0.29	18
$2\nu_2^0+\nu_4^1$	F_2	4348.72	4348.07	0.65	5
$2\nu_2^2+\nu_4^1$	F_1	4363.62	4362.86	0.76	18
$2\nu_2^2+\nu_4^1$	F_2	4378.94	4378.30	0.64	18
$\nu_1+\nu_2^1$	E	4435.13	4435.25	−0.12	18
$\nu_2^1+\nu_3^1$	F_1	4537.55	4538.13	−0.58	5
$\nu_2^1+\nu_3^1$	F_2	4543.76	4544.36	−0.60	5
$3\nu_2^1$	E	4592.03	4591.08	0.95	5
$3\nu_2^3$	A_2	4595.28	4594.40	0.88	18
$3\nu_2^3$	A_1	4595.52	4594.49	1.03	18
$4\nu_4^0$	A_1	5121.77	5121.51[a]	0.26	26
$4\nu_4^2$	F_2	5143.36	5143.07[a]	0.29	18
$4\nu_4^2$	E	5167.20	5167.15[a]	0.05	18
$4\nu_4^4$	F_2	5210.74	5209.06[a]	1.68	18
$4\nu_4^4$	E	5228.74	5227.45[a]	1.29	18
$4\nu_4^4$	F_1	5230.59	5229.46[a]	1.13	26
$4\nu_4^4$	A_1	5240.46	5239.76[a]	0.70	26
$\nu_2^1+3\nu_4^1$	F_2	5370.48	5369.79	0.69	26
$\nu_2^1+3\nu_4^1$	F_1	5389.74	5388.96	0.78	26
$\nu_2^1+3\nu_4^1$	E	5424.80	5423.39	1.41	26
$\nu_2^1+3\nu_4^3$	F_2	5429.86	5428.85	1.01	26
$\nu_2^1+3\nu_4^3$	F_1	5437.28	5436.38	0.90	26
$\nu_2^1+3\nu_4^3$	F_2	5444.80	5444.07	0.73	18
$\nu_2^1+3\nu_4^3$	F_1	5462.91	5461.86	1.05	26
$\nu_1+2\nu_4^0$	A_1	5492.90	5492.32	0.58	26
$\nu_3^1+2\nu_4^0$	F_2	5587.97	5587.97	0.00	18

TABLE II. (*Continued.*)

Mode	Sym.	Experiment	Calculated	Obs–calc	Reference
$\nu_3^1+2\nu_4^2$	A_1	5604.47	5604.51	−0.04	18
$2\nu_2^0+2\nu_4^0$	A_1	5613.88	5612.61	1.27	26[b]
$2\nu_2^2+2\nu_4^0$	E	5614.58	5613.15	1.43	26
$\nu_3^1+2\nu_4^2$	F_1	5615.37	5615.75	−0.38	26
$\nu_3^1+2\nu_4^2$	F_2	5616.02	5615.46	0.56	26
$\nu_3^1+2\nu_4^2$	E	5618.23	5618.85	−0.62	26
$\nu_3^1+2\nu_4^2$	F_1	5626.10	5626.96	−0.86	26
$\nu_3^1+2\nu_4^2$	F_2	5627.35	5628.29	−0.94	26
$2\nu_2^0+2\nu_4^2$	F_2	5641.88	5641.63	0.25	26
$2\nu_2^2+2\nu_4^2$	E	5654.47	5653.58	0.89	26
$2\nu_2^2+2\nu_4^2$	F_1	5655.76	5655.28	0.48	18
$2\nu_2^2+2\nu_4^2$	A_2	5664.08	5663.38	0.70	26
$2\nu_2^0+2\nu_4^2$	F_2	5668.33	5668.25	0.08	26
$2\nu_2^2+2\nu_4^2$	A_1	5681.26	5681.25	0.01	26
$2\nu_2^0+2\nu_4^2$	E	5691.10	5690.32	0.78	26
$2\nu_1$	A_1	5790.25	5792.08	−1.83	86
$\nu_2^1+\nu_3^1+\nu_4^1$	F_2	5823.10	5823.65	−0.55	18
$\nu_2^1+\nu_3^1+\nu_4^1$	F_1	5825.43	5825.59	−0.16	26
$\nu_2^1+\nu_3^1+\nu_4^1$	E	5832.02	5832.60	−0.58	18
$\nu_2^1+\nu_3^1+\nu_4^1$	A_1	5834.82	5835.64	−0.82	18
$\nu_2^1+\nu_3^1+\nu_4^1$	E	5842.57	5843.12	−0.55	26
$\nu_2^1+\nu_3^1+\nu_4^1$	A_2	5843.19	5843.83	−0.64	26
$\nu_2^1+\nu_3^1+\nu_4^1$	F_2	5844.03	5844.28	−0.25	18
$\nu_2^1+\nu_3^1+\nu_4^1$	F_1	5847.39	5847.66	−0.27	26
$\nu_1+\nu_3^1$	F_2	5861.49	5861.90	−0.41	18
$3\nu_2^1+\nu_4^1$	F_2	5867.52	5868.09	−0.57	26
$3\nu_2^3+\nu_4^1$	F_1	5879.80	5878.97	0.83	26
$3\nu_2^3+\nu_4^1$	F_2	5894.34	5893.51	0.83	26
$3\nu_2^1+\nu_4^1$	F_1	5908.74	5908.52	0.22	26
$\nu_1+2\nu_2^2$	E	5952.44	5952.00	0.44	18
$2\nu_3^0$	A_1	5968.15	5969.12	−0.97	87
$2\nu_3^2$	F_2	6004.62	6006.54	−1.92	18
$2\nu_3^2$	E	6043.82	6046.12	−2.30	18
$2\nu_2^0+\nu_3^1$	F_2	6054.61	6054.74	−0.13	18
$2\nu_2^2+\nu_3^1$	F_1	6060.62	6060.67	−0.05	18
$2\nu_2^2+\nu_3^1$	F_2	6065.59	6065.48	0.11	18
$4\nu_2^2$	E	6118.95	6117.21	1.74	26
$4\nu_2^4$	E	6124.12	6122.77	1.35	26

[a] $P_{\max} = 14$ value.
[b] Assigned as $\nu_3+2\nu_4$ in TROVE.

TABLE III. Six $J = 0$ vibrational term values (in cm^{-1}) in the tetradecad region which have a large experimental uncertainty (see text). Comparisons are given with the CBS-F12^{HL} PES (this work), the empirically refined PES of Wang and Carrington[47] (denoted as WC), and the empirically adjusted PES of Nikitin *et al.*[44] (denoted as NRT).

Mode	Sym.	Experiment[18]	CBS-F12^{HL}	WC	NRT
$\nu_1+2\nu_4^2$	F_2	5519.88	5520.95	5522.32	5522.66
$\nu_1+2\nu_4^2$	E	5536.23	5533.62	5534.54	5534.20
$\nu_1+\nu_2^1+\nu_4^1$	F_2	5728.58	5726.71	5727.50	5727.72
$\nu_1+\nu_2^1+\nu_4^1$	F_1	5745.90	5744.72	5745.78	5745.31
$\nu_1+2\nu_2^0$	A_1	5945.81	5940.11	5939.90	5939.96
$4\nu_2^0$	A_1	6122.13	6115.42	6116.74	6117.75

TABLE IV. Comparison of calculated and experimental $J = 0$ vibrational term values (in cm^{-1}) for $^{12}CH_4$ in the icosad region (see text for a discussion of the experimental uncertainties). The zero-point energy was computed to be 9708.846 cm^{-1} at the CVBS limit.

Mode	Sym.	Experiment	Calculated	Obs–calc	Reference
$5\nu_4^1$	F_2	6450.06	6449.72	0.34	13
$5\nu_4^5$	F_2	6507.55	6505.66	1.89	13
$5\nu_4^5$	F_2	6539.18	6538.17	1.01	13
$\nu_2^1+4\nu_4^2$	F_2	6657.09	6657.88[a]	−0.79	24
$\nu_2^1+4\nu_4^4$	F_2	6717.99	6715.72	2.27	25
$\nu_2^1+4\nu_4^4$	F_2	6733.11	6731.87	1.24	25
$\nu_1+3\nu_4^1$	F_2	6769.19	6769.51	−0.32	25
$\nu_1+3\nu_4^3$	F_2	6833.19	6833.46	−0.27	25
$\nu_3^1+3\nu_4^1$	F_2	6858.71	6858.84	−0.13	25
$2\nu_2^0+3\nu_4^1$	F_2	6869.79	6869.70	0.09	25
$\nu_3^1+3\nu_4^3$	F_2	6897.38	6896.88	0.50	25
$\nu_3^1+3\nu_4^1$	F_2	6910.38	6910.46	−0.08	25
$\nu_3^1+3\nu_4^1$	F_2	6924.97	6925.69	−0.72	25
$2\nu_2^2+3\nu_4^3$	F_2	6940.05	6939.69	0.36	24
$2\nu_2^2+3\nu_4^3$	F_2	6992.58	6992.15	0.43	25
$\nu_1+\nu_2^1+2\nu_4^2$	F_2	7035.18	7035.07	0.11	25
$2\nu_1+\nu_4^1$	F_2	7085.64	7086.77	−1.13	25
$\nu_2^1+\nu_3^1+2\nu_4^0$	F_2	7097.92	7098.61	−0.69	25[b]
$\nu_2^1+\nu_3^1+2\nu_4^2$	F_2	7116.39	7117.01	−0.62	25
$\nu_2^1+\nu_3^1+2\nu_4^2$	F_2	7131.14	7131.56	−0.42	25
$\nu_1+\nu_3^1+\nu_4^1$	F_2	7158.13	7159.05	−0.92	25[c]
$3\nu_2^3+2\nu_4^2$	F_2	7168.42	7168.23	0.19	25
$\nu_1+2\nu_2^2+\nu_4^1$	F_2	7225.43	7225.49	−0.06	25
$2\nu_3^0+\nu_4^1$	F_2	7250.54	7251.24	−0.70	25
$\nu_1+2\nu_2^0+\nu_4^1$	F_2	7269.44	7269.68	−0.24	25
$2\nu_3^2+\nu_4^1$	F_2	7299.44	7300.72	−1.28	25
$2\nu_2^0+\nu_3^1+\nu_4^1$	F_2	7331.05	7331.69	−0.64	25
$2\nu_2^2+\nu_3^1+\nu_4^1$	F_2	7346.01	7346.10	−0.10	25
$2\nu_2^2+\nu_3^1+\nu_4^1$	F_2	7365.40	7365.35	0.05	25
$\nu_1+\nu_2^1+\nu_3^1$	F_2	7374.25	7374.42	−0.17	25
$4\nu_2^2+\nu_4^1$	F_2	7384.11	7384.03	0.08	25
$\nu_2^1+2\nu_3^2$	F_2	7510.34	7511.56	−1.22	1
$3\nu_2^1+\nu_3^1$	F_2	7575.86	7575.43	0.43	25
$3\nu_2^3+\nu_3^1$	F_2	7584.51	7583.50	1.01	25

[a] $P_{max} = 14$ value.
[b] Assigned as $2\nu_1+\nu_4$ in TROVE.
[c] Value of 7156.72 cm^{-1} reported by Ulenikov *et al.*[20]

relate to primitive basis functions ϕ_{n_k}, which are obtained by solving a one-dimensional Schrödinger equation for each kth vibrational mode using the Numerov-Cooley method.[81,82] Multiplication with symmetrized rigid-rotor eigenfunctions $|J, \Gamma_{rot}, n\rangle$ gives the final basis set for use in $J > 0$ calculations. The label Γ_{rot} is the rotational symmetry and n is a multiplicity index used to count states within a given J (see the work of Boudon *et al.*[3]).

In TROVE the eigenvalues and corresponding eigenvectors are assigned with quantum numbers based on the contribution of the basis functions ϕ_{n_k}. To be of spectroscopic use it is necessary to map these to the normal mode quantum numbers v_k commonly used. For CH_4, vibrational states are labelled as $v_1\nu_1 + v_2\nu_2^{L_2} + v_3\nu_3^{L_3} + v_4\nu_4^{L_4}$, where v_i counts the level of excitation. The additional quantum numbers L_i are the absolute values of the vibrational angular momentum quantum numbers ℓ_i, which are needed to resolve the degeneracy of their respective modes (see the work of Yurchenko and Tennyson[46] for further details). The non-degenerate symmetric stretching mode ν_1 (2916.48 cm^{-1}) is of A_1 symmetry. The doubly degenerate asymmetric bending mode ν_2 (1533.33 cm^{-1}) has E symmetry. Whilst of F_2 symmetry are the triply degenerate modes; the asymmetric stretching mode ν_3 (3019.49 cm^{-1}) and the asymmetric bending mode ν_4 (1310.76 cm^{-1}). The values in parentheses are the experimentally determined values.[5]

TABLE V. Comparison of calculated and experimental $J = 0$ vibrational term values (in cm^{-1}) for $^{12}CH_4$ in the icosad region and above (see text for a discussion of the experimental uncertainties). The zero-point energy was computed to be 9708.846 cm^{-1} at the CVBS limit.

Mode	Sym.	Experiment	Calculated	Obs–calc	Reference
$5\nu_4^5$	F_2	6377.53	6381.09[a]	−3.56	13
$5\nu_4^1$	A_1	6405.89	6410.06[a]	−4.17	25
$5\nu_4^3$	F_1	6429.20	6428.63	0.57	25
$5\nu_4^3$	E	6507.37	6505.12	2.25	25
$5\nu_4^5$	F_1	6529.74	6528.34	1.40	25
$\nu_2^1+4\nu_4^0$	E	6617.50	6615.81	1.69	25
$\nu_2^1+4\nu_4^2$	F_1	6638.52	6636.01	2.51	25
$\nu_2^1+4\nu_4^2$	A_1	6655.88	6655.99	−0.11	25
$\nu_2^1+4\nu_4^2$	E	6680.93	6680.84	0.09	24
$\nu_2^1+4\nu_4^4$	A_2	6682.82	6681.55	1.27	25
$\nu_2^1+4\nu_4^4$	F_1	6722.00	6719.33	2.67	25
$\nu_2^1+4\nu_4^4$	E	6729.60	6728.27	1.33	24
$\nu_2^1+4\nu_4^4$	A_1	6737.79	6737.18	0.61	25
$\nu_2^1+4\nu_4^2$	A_2	6746.23	6745.40	0.83	25
$\nu_2^1+4\nu_4^4$	F_1	6755.38	6754.15	1.23	25
$\nu_2^1+4\nu_4^4$	E	6766.23	6765.13	1.10	24
$\nu_1+3\nu_4^1$	A_1	6809.40	6808.77	0.63	25
$\nu_1+3\nu_4^3$	F_1	6822.30	6821.92	0.38	25
$\nu_3^1+3\nu_4^1$	E	6862.74	6863.53	−0.79	25
$\nu_3^1+3\nu_4^1$	F_1	6862.85	6863.20	−0.35	24
$\nu_3^1+3\nu_4^1$	A_1	6863.10	6864.32	−1.22	25
$2\nu_2^2+3\nu_4^1$	F_1	6889.68	6889.53	0.15	25
$2\nu_2^2+3\nu_4^3$	F_2	6905.60	6905.65	−0.05	25
$\nu_3^1+3\nu_4^3$	E	6908.80	6908.84	−0.04	25
$\nu_3^1+3\nu_4^3$	F_1	6915.18	6915.22	−0.04	25
$\nu_3^1+3\nu_4^3$	A_2	6918.55	6918.95	−0.40	25
$\nu_3^1+3\nu_4^3$	F_1	6921.58	6921.75	−0.17	25
$\nu_3^1+3\nu_4^3$	A_1	6922.07	6923.24	−1.17	25
$\nu_3^1+3\nu_4^3$	E	6925.67	6927.00	−1.33	25
$2\nu_2^2+3\nu_4^1$	E	6938.40	6937.71	0.69	25
$2\nu_2^0+3\nu_4^1$	A_1	6940.10	6939.47	0.63	25
$2\nu_2^0+3\nu_4^3$	F_1	6945.16	6944.87	0.29	24
$2\nu_2^2+3\nu_4^3$	F_1	6949.70	6949.57	0.13	25
$2\nu_2^0+3\nu_4^3$	F_2	6962.42	6962.61	−0.19	25
$\nu_1+\nu_2^1+2\nu_4^0$	E	6990.01	6990.06	−0.05	25
$\nu_1+\nu_2^1+2\nu_4^2$	F_1	7020.43	7020.19	0.24	25
$\nu_1+\nu_2^1+2\nu_4^2$	A_1	7024.03	7024.05	−0.02	25
$\nu_1+\nu_2^1+2\nu_4^2$	E	7045.69	7045.89	−0.20	25
$\nu_1+\nu_2^0+2\nu_4^2$	A_2	7056.56	7056.50	0.06	25
$\nu_2^1+\nu_3^1+2\nu_4^0$	F_1	7085.73	7085.45	0.28	25
$\nu_2^1+\nu_3^1+2\nu_4^0$	E	7107.28	7107.39	−0.11	25
$\nu_2^1+\nu_3^1+2\nu_4^2$	A_2	7114.54	7114.43	0.11	25
$3\nu_2^1+2\nu_4^0$	E	7118.40	7118.32	0.08	25
$3\nu_2^3+2\nu_4^0$	A_1	7120.74	7120.58	0.16	25
$\nu_2^1+\nu_3^1+2\nu_4^2$	F_2	7121.90	7122.10	−0.20	25
$\nu_2^1+\nu_3^1+2\nu_4^2$	F_1	7130.90	7131.40	−0.50	25
$\nu_2^1+\nu_3^1+2\nu_4^2$	A_1	7132.50	7132.71	−0.21	25
$3\nu_2^3+2\nu_4^0$	A_2	7133.69	7133.51	0.18	25
$\nu_2^1+\nu_3^1+2\nu_4^2$	E	7134.00	7134.10	−0.10	25
$\nu_2^1+\nu_3^1+2\nu_4^2$	F_1	7139.23	7140.33	−1.10	25
$\nu_2^1+\nu_3^1+2\nu_4^2$	F_2	7141.50	7142.22	−0.72	25
$\nu_2^1+\nu_3^1+2\nu_4^2$	F_1	7151.02	7151.08	−0.06	25
$3\nu_2^1+2\nu_4^2$	F_1	7153.84	7153.86	−0.02	25

TABLE V. (*Continued.*)

Mode	Sym.	Experiment	Calculated	Obs–calc	Reference
$\nu_1+\nu_3^1+\nu_4^1$	A_1	7157.16	7158.06	−0.90	25
$\nu_1+\nu_3^1+\nu_4^1$	E	7164.60	7165.63	−1.03	25
$\nu_1+\nu_3^1+\nu_4^1$	F_1	7165.60	7167.95	−2.35	25
$3\nu_2^3+2\nu_4^2$	E	7168.00	7168.62	−0.62	25[b]
$3\nu_2^1+2\nu_4^2$	A_1	7176.10	7176.09	0.01	25
$3\nu_2^3+2\nu_4^2$	F_1	7180.00	7180.01	−0.01	25
$3\nu_2^1+2\nu_4^2$	F_2	7191.05	7191.12	−0.07	25
$3\nu_2^3+2\nu_4^2$	E	7191.85	7191.45	0.40	25
$3\nu_2^1+2\nu_4^2$	E	7217.40	7217.22	0.18	25
$3\nu_2^1+2\nu_4^2$	A_2	7221.10	7220.74	0.36	25
$\nu_1+2\nu_2^2+\nu_4^1$	F_1	7246.01	7245.65	0.36	25
$2\nu_1+\nu_2^1$	E	7295.20	7296.34	−1.14	25
$2\nu_3^2+\nu_4^1$	E	7295.50	7298.40	−2.90	25
$2\nu_3^2+\nu_4^1$	F_1	7295.80	7297.66	−1.86	25
$2\nu_3^2+\nu_4^1$	A_1	7299.45	7300.32	−0.87	25
$2\nu_2^2+\nu_3^1+\nu_4^1$	F_1	7326.25	7326.94	−0.69	25
$2\nu_3^2+\nu_4^1$	F_2	7337.55	7339.75	−2.20	25
$2\nu_3^2+\nu_4^1$	F_1	7338.16	7340.03	−1.87	25
$2\nu_2^0+\nu_3^1+\nu_4^1$	A_1	7341.60	7341.87	−0.27	25
$2\nu_2^2+\nu_3^1+\nu_4^1$	E	7342.10	7342.38	−0.28	25
$2\nu_2^2+\nu_3^1+\nu_4^1$	F_1	7346.46	7346.66	−0.20	25
$2\nu_2^2+\nu_3^1+\nu_4^1$	A_2	7348.85	7349.29	−0.44	25
$2\nu_2^2+\nu_3^1+\nu_4^1$	E	7352.20	7352.48	−0.28	25
$2\nu_2^2+\nu_3^1+\nu_4^1$	A_1	7360.80	7361.31	−0.51	25
$2\nu_2^0+\nu_3^1+\nu_4^1$	F_1	7368.88	7368.97	−0.09	25
$\nu_1+\nu_2^1+\nu_3^1$	F_1	7373.16	7373.97	−0.81	25
$4\nu_2^2+\nu_4^1$	F_1	7394.20	7393.64	0.56	25
$4\nu_2^4+\nu_4^1$	F_2	7408.20	7407.40	0.80	25
$4\nu_2^4+\nu_4^1$	F_1	7422.30	7421.35	0.95	25
$4\nu_2^2+\nu_4^1$	F_2	7436.30	7435.90	0.40	25
$\nu_1+3\nu_2^1$	E	7447.52	7447.83	−0.31	25
$\nu_1+3\nu_2^3$	A_2	7468.21	7467.33	0.88	25
$\nu_1+3\nu_2^3$	A_1	7468.50	7467.42	1.08	25
$\nu_2^1+2\nu_3^0$	E	7483.67	7483.79	−0.12	25
$\nu_2^1+2\nu_3^2$	F_1	7512.26	7513.39	−1.13	25
$\nu_2^1+2\nu_3^2$	E	7552.23	7553.79	−1.56	25
$\nu_2^1+2\nu_3^2$	A_1	7559.00	7560.60	−1.60	25
$3\nu_2^1+\nu_3^1$	F_1	7569.51	7569.25	0.26	25
$3\nu_2^3+\nu_3^1$	F_1	7580.90	7580.36	0.54	25
$2\nu_1+2\nu_4^2$	F_2	8388.00	8384.52	3.48	20
$\nu_1+\nu_3^1+2\nu_4^2$	F_2	8421.00	8422.37	−1.37	20
$\nu_1+2\nu_3^2$	F_2	8618.67	8613.92	4.75	20
$2\nu_1+\nu_3$	F_2	8808.95	8812.01[a,c]	−3.06	20
$3\nu_3^1$	F_2	8907.30	8909.59	−2.29	20
$3\nu_3^3$	F_2	9045.96	9048.87	−2.91	20
$\nu_1+2\nu_3^0+\nu_4^1$	F_2	9888.47	9892.46[a]	−3.99	20
$\nu_1+\nu_2+2\nu_3$	F_2	10115.67	[d]	...	20
$3\nu_3+\nu_4$	F_2	10265.59	[d]	...	20
$2\nu_1+\nu_2+\nu_3$	F_2	10302.17	[d]	...	20
$\nu_1+3\nu_3$	F_2	11276.31	11277.96[c]	−1.65	20

[a] $P_{max} = 14$ value.
[b] Assigned as $\nu_1+\nu_3+\nu_4$ in TROVE.
[c] Unable to identify vibrational angular momentum quantum numbers.
[d] Unable to identify energy level in TROVE.

IV. RESULTS

A. Vibrational $J = 0$ energy levels

A reliable assessment of the CBS-F12^{HL} PES is only possible with converged vibrational term values. Calculations with $P_{max} = 14$ are sufficient for converging low-lying states but this gradually deteriorates as we go up in energy. A way of overcoming this problem is to employ a complete vibrational basis set (CVBS) extrapolation.[55] Similar to basis set extrapolation techniques of electronic structure theory,[83,84] the same approach can be applied to TROVE calculations with respect to P_{max}. We use the exponential decay expression,

$$E_i(P_{max}) = E_i^{CVBS} + A_i \exp(-\lambda_i P_{max}), \quad (13)$$

where E_i is the energy of the ith level, E_i^{CVBS} is the corresponding energy at the CVBS limit, A_i is a fitting parameter, λ_i is determined from

$$\lambda_i = -\frac{1}{2} \ln \left(\frac{E_i(P_{max}+2) - E_i(P_{max})}{E_i(P_{max}) - E_i(P_{max}-2)} \right) \quad (14)$$

and the values of $P_{max} = \{10, 12, 14\}$.

Briefly commenting on the accuracy of the CVBS extrapolation itself, similar to electronic structure theory the use of larger basis sets is always preferable for the extrapolation. Highly excited modes benefit the most as convergence is much slower, however, at higher energies the increased density of states makes it harder to consistently identify and match energy levels for different values of P_{max}. To ensure a reliable extrapolation we have also found that $\lambda_i \geq 0.5$.

In the following comparisons we have collected, to the best of our knowledge, all $J = 0$ energies that have been accurately determined from experiment (see the work of Manca *et al.*[85] for a discussion of the experimental uncertainties associated with methane spectra). Although very minor discrepancies occasionally occur between different studies, the majority of vibrational term values up to the tetradecad region (up to 6300 cm^{-1}) are fairly well established. Progress is being made in the icosad range (6300–7900 cm^{-1}) and a large number of levels have recently been assigned[24,25] using the WKLMC line list.[28] At even higher energies several vibrational band centers have been measured and assigned by means of an assignment of their P(1) transitions up to about 11 300 cm^{-1}.[20]

Computed vibrational energy levels for $^{12}CH_4$ up to the tetradecad region are listed in Table II. The four fundamentals are reproduced with a rms error of 0.70 cm^{-1} and a mean-absolute-deviation (mad) of 0.64 cm^{-1}. Around 70% of the 89 term values are calculated within spectroscopic accuracy (better than ±1 cm^{-1}) and this does not include the $4\nu_4$ levels computed at $P_{max} = 14$, which are not fully converged.

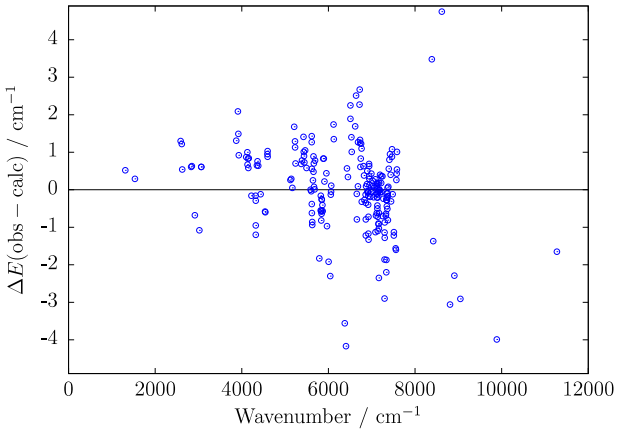

FIG. 2. Residual errors ΔE(obs – calc) for all computed term values of $^{12}CH_4$ (see Tables II, IV, and V).

Six energy levels in the tetradecad region have not been included in Table II because their experimental uncertainty could be as large as 5 cm^{-1} (see Nikitin *et al.*[18]). Instead they are listed in Table III alongside computed values from the CBS-F12^{HL} PES, the empirically refined PES of Wang and Carrington[47] (denoted as WC), and the empirically adjusted PES of Nikitin *et al.*[44] (denoted as NRT). The three PESs show consistent agreement with each other, notably for the $\nu_1 + 2\nu_2^0(A_1)$ and $4\nu_2^0(A_1)$ levels where the residual errors, ΔE(obs – calc), compared to Nikitin *et al.*[18] are the largest. This would suggest that the effective Hamiltonian model used in Nikitin *et al.*[18] and subsequently updated by Amyay *et al.*[26] may need further refinement in the tetradecad region.

For the icosad region and above, shown in Tables IV and V, spectroscopic accuracy is again achieved for around 70% of the 134 term values considered. Here we have separated the computed energies into two separate tables based on the accuracy of the corresponding values from experiment, which are predominantly from Refs. 13, 24, and 25. The values in Table IV have an experimental accuracy of 0.0015 cm^{-1} (the $\nu_2^1 + 2\nu_3^2$ level from Hippler and Quack[1] has an uncertainty of 0.0010 cm^{-1}). In Table V, energies have an accuracy of 0.1–0.4 cm^{-1}, except for the vibrational band centers from Ulenikov *et al.*[20] which have a reported

TABLE VI. Equilibrium C–H bond length.

r (C–H) / Å	Reference	Approach
1.08601	This work	Purely *ab initio* PES
1.08598	This work	Refined geometry PES
1.08601(4)	44	Empirically adjusted PES
1.08609	47	Empirically refined PES
1.08595(30)	88	Combined experimental and *ab initio* analysis
1.086(2)	89	Quantum Monte Carlo calculations
1.0847	5	Effective Hamiltonian model
1.08553(4)	26	Effective Hamiltonian model

TABLE VII. Comparison of calculated and experimental $J \leq 10$ pure rotational energy levels (in cm^{-1}) for $^{12}CH_4$. The experimental ground state values are from the work of Nikitin *et al.*[44] but are originally attributed to the spherical top data system.[90] Computed values correspond to the *ab initio* geometry (A) and the empirically refined geometry (B) (see text).

J	K	Sym.	Experiment	Calculated (A)	Calculated (B)	Obs–calc (A)	Obs–calc (B)
0	0	A_1	0.00000	0.00000	0.00000	0.00000	0.00000
1	1	F_1	10.48165	10.48105	10.48164	0.00060	0.00001
2	1	F_2	31.44239	31.44061	31.44235	0.00178	0.00004
2	2	E	31.44212	31.44034	31.44209	0.00178	0.00003
3	1	F_2	62.87684	62.87329	62.87678	0.00355	0.00006
3	2	A_2	62.87817	62.87462	62.87811	0.00355	0.00006
3	3	F_1	62.87578	62.87222	62.87571	0.00356	0.00007
4	0	A_1	104.77284	104.76692	104.77274	0.00592	0.00010
4	1	F_1	104.77470	104.76879	104.77460	0.00591	0.00010
4	2	E	104.77603	104.77012	104.77594	0.00591	0.00009
4	3	F_2	104.78001	104.77411	104.77993	0.00590	0.00008
5	1	F_1	157.12434	157.11548	157.12420	0.00886	0.00014
5	2	E	157.13719	157.12837	157.13709	0.00882	0.00010
5	3	F_1	157.13892	157.13010	157.13882	0.00882	0.00010
5	5	F_2	157.12793	157.11908	157.12780	0.00885	0.00013
6	1	F_2	219.91505	219.90268	219.91487	0.01237	0.00018
6	2	A_2	219.91985	219.90750	219.91969	0.01235	0.00016
6	3	F_1	219.94126	219.92897	219.94117	0.01229	0.00009
6	4	A_1	219.94523	219.93295	219.94515	0.01228	0.00008
6	5	F_2	219.93677	219.92446	219.93666	0.01231	0.00011
6	6	E	219.91346	219.90109	219.91328	0.01237	0.00018
7	1	F_1	293.12299	293.10652	293.12277	0.01647	0.00022
7	1	F_2	293.12655	293.11010	293.12634	0.01645	0.00021
7	2	A_2	293.15420	293.13783	293.15408	0.01637	0.00012
7	3	F_2	293.16457	293.14823	293.16448	0.01634	0.00009
7	5	F_1	293.17868	293.16238	293.17864	0.01630	0.00004
7	6	E	293.17013	293.15381	293.17007	0.01632	0.00006
8	0	A_1	376.73044	376.70932	376.73019	0.02112	0.00025
8	1	F_1	376.73372	376.71261	376.73349	0.02111	0.00023
8	2	E	376.82129	376.80044	376.82133	0.02085	−0.00004
8	3	F_1	376.80478	376.78388	376.80476	0.02090	0.00002
8	3	F_2	376.82627	376.80544	376.82632	0.02083	−0.00005
8	5	F_2	376.78587	376.76492	376.78581	0.02095	0.00006
8	6	E	376.73565	376.71454	376.73541	0.02111	0.00024
9	1	F_1	470.71696	470.69064	470.71670	0.02632	0.00026
9	1	F_2	470.72034	470.69403	470.72009	0.02631	0.00025
9	2	E	470.79897	470.77290	470.79898	0.02607	−0.00001
9	3	F_1	470.80528	470.77923	470.80531	0.02605	−0.00003
9	4	A_1	470.83096	470.80498	470.83106	0.02598	−0.00010
9	5	F_2	470.86506	470.83918	470.86528	0.02588	−0.00022
9	6	A_2	470.87292	470.84707	470.87315	0.02585	−0.00023
9	7	F_1	470.85500	470.82910	470.85517	0.02590	−0.00017
10	1	F_1	575.18430	575.15264	575.18447	0.03166	−0.00017
10	1	F_2	575.05266	575.02059	575.05242	0.03207	0.00024
10	2	A_2	575.05567	575.02361	575.05544	0.03206	0.00023
10	3	F_2	575.17008	575.13837	575.17019	0.03171	−0.00011
10	5	F_1	575.25978	575.22834	575.26020	0.03144	−0.00042
10	6	E	575.27192	575.24050	575.27236	0.03142	−0.00044
10	7	F_2	575.28542	575.25405	575.28589	0.03137	−0.00047
10	8	A_1	575.22292	575.19137	575.22321	0.03155	−0.00029
10	10	E	575.05127	575.01920	575.05101	0.03207	0.00026

experimental uncertainty of around 0.001 cm^{-1}; a result of the direct method used. However, the $\nu_1 + \nu_3^l + \nu_4^l(F_2)$ level from Ulenikov *et al.*[20] shows a discrepancy of 1.41 cm^{-1} compared to the recent value published by Rey *et al.*[25]

Three term values from Ulenikov *et al.*[20] above 10 000 cm^{-1} could not be confidently identified in TROVE. The increased density of states and approximate TROVE labelling scheme can make it difficult to unambiguously discern

certain levels. Regardless, from Tables IV and V it is evident that the CBS-F12^{HL} PES provides a reliable description at higher energies and there does not appear to be any significant deterioration in accuracy (see Fig. 2 for an overview of the residual errors for all term values). This will be important for investigating methane spectra up to the 14 000 cm^{-1} region, which is a key motivation for the present work.

B. Equilibrium geometry and pure rotational energies

The value of r_{ref} used in Eq. (3) does not define the minimum of the PES because a linear expansion term has been included in the parameter set. The true equilibrium C–H bond length determined from the CBS-F12^{HL} PES is listed in Table VI. It is in excellent agreement with previous values which is gratifying as it has been calculated in a purely *ab initio* fashion.

However, it is more informative to look at pure rotational energies as these are highly dependent on the molecular geometry through the moments of inertia. In Table VII, computed rotational energy levels up to $J = 10$ are compared against experimental values listed in the work of Nikitin *et al.*[44] (originally attributed to the spherical top data system,[90] which contains measurements from Oldani *et al.*[91]). Calculations were carried out with $P_{max} = 12$ which is sufficient for converging ground state rotational energies.

The CBS-F12^{HL} PES consistently underestimates ground state rotational energy levels and the residual error increases systematically by about 0.00060 cm^{-1} at each step up in J. Overall, the 51 energies are reproduced with a rms error of 0.02008 cm^{-1}. This is around two orders of magnitude larger than the empirically adjusted PES of Nikitin *et al.*[44] which yields an identical value of r (C–H) = 1.08601 Å for the C–H bond length but a rms error of 0.00029 cm^{-1}.

To help explain this discrepancy it is relatively straightforward to improve the CBS-F12^{HL} results by refining the equilibrium geometry. This is done through a nonlinear least-squares fitting to the experimental energy levels and can significantly improve the accuracy of computed intra-band rotational wavenumbers.[34,80,92] After two iterations refining the parameter r_{ref}, the experimental energy levels up to $J = 10$ are reproduced with a rms error of 0.00018 cm^{-1} (see Table VII and Fig. 3) and this corresponds to a bond length of r (C–H) = 1.08598 Å (also given in Table VI). This value is within the uncertainty of the bond length from the work of Nikitin *et al.*[44] and is remarkably close to the original *ab initio* result. However, we have refrained from adopting the new equilibrium geometry for the CBS-F12^{HL} PES as it leads to a poorer description of vibrational energies (see, for example, Ref. 34), which were the main focus of this work.

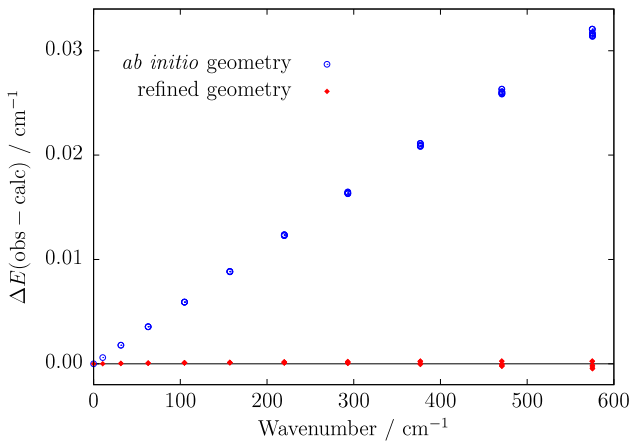

FIG. 3. Residual errors ΔE(obs − calc) for computed pure rotational energies using the *ab initio* and empirically refined equilibrium geometry (see Table VII).

V. CONCLUSIONS

State-of-the-art electronic structure calculations have been used to generate a new nine-dimensional PES for methane. The CBS-F12^{HL} PES represents the most accurate *ab initio* surface to date. This is confirmed by the achievement of sub-wavenumber accuracy for a considerable number of vibrational energy levels including those at higher energies. Although the computed *ab initio* equilibrium C–H bond length was in excellent agreement with previous values, systematic errors arose in calculated pure rotational energies of $^{12}CH_4$. These errors could be significantly reduced by adjusting the equilibrium geometry of the CBS-F12^{HL} PES. The resultant bond length was remarkably close to the original *ab initio* value and still consistent with prior studies.

Despite the advances in electronic structure theory, the best *ab initio* PES is rarely accurate enough for the requirements of high-resolution spectroscopy and empirical refinement is a necessary step. Refinement can be a computationally intensive process[93] but it can produce orders-of-magnitude improvements in the accuracy of computed rovibrational energy levels. It is natural then to question the benefit of using sophisticated methods with large basis sets to generate the original *ab initio* surface. Whilst a better *ab initio* PES will lead to a superior refinement, at some stage the gain in accuracy when simulating rotation-vibration spectra will not correlate with the computational cost of improving the underlying *ab initio* surface. For this reason we believe that more sophisticated electronic structure calculations to improve the CBS-F12^{HL} PES are currently not worthwhile. The CBS-F12^{HL} PES will serve as an excellent starting point for refinement and we recommend this surface for future use.

SUPPLEMENTARY MATERIAL

See supplementary material for the expansion parameters and corresponding program to construct the CBS-F12^{HL} PES. A list of computed vibrational $J = 0$ energy levels of $^{12}CH_4$ is also provided.

ACKNOWLEDGMENTS

This work was supported by ERC Advanced Investigator Project No. 267219 and FP7-MC-IEF Project No. 629237.

[1]M. Hippler and M. Quack, J. Chem. Phys. **116**, 6045 (2002).
[2]L. R. Brown, J. Quant. Spectrosc. Radiat. Transfer **96**, 251 (2005).

[3]V. Boudon, M. Rey, and M. Loëte, J. Quant. Spectrosc. Radiat. Transfer **98**, 394 (2006).
[4]S. Kassi, B. Gao, D. Romanini, and A. Campargue, Phys. Chem. Chem. Phys. **10**, 4410 (2008).
[5]S. Albert, S. Bauerecker, V. Boudon, L. R. Brown, J. P. Champion, M. Loëte, A. Nikitin, and M. Quack, Chem. Phys. **356**, 131 (2009).
[6]S. Kassi, D. Romanini, and A. Campargue, Chem. Phys. Lett. **477**, 17 (2009).
[7]E. Sciamma-O'Brien, S. Kassi, B. Gao, and A. Campargue, J. Quant. Spectrosc. Radiat. Transfer **110**, 951 (2009).
[8]O. Votava, M. Masat, P. Pracna, S. Kassi, and A. Campargue, Phys. Chem. Chem. Phys. **12**, 3145 (2010).
[9]A. Campargue, L. Wang, S. Kassi, M. Mašát, and O. Votava, J. Quant. Spectrosc. Radiat. Transfer **111**, 1141 (2010).
[10]L. Wang, S. Kassi, A. W. Liu, S. M. Hu, and A. Campargue, J. Mol. Spectrosc. **261**, 41 (2010).
[11]Y. Lu, D. Mondelain, S. Kassi, and A. Campargue, J. Quant. Spectrosc. Radiat. Transfer **112**, 2683 (2011).
[12]D. Mondelain, S. Kassi, L. Wang, and A. Campargue, Phys. Chem. Chem. Phys. **13**, 7985 (2011).
[13]A. V. Nikitin, X. Thomas, L. Regalia, L. Daumont, P. Von der Heyden, V. G. Tyuterev, L. Wang, S. Kassi, and A. Campargue, J. Quant. Spectrosc. Radiat. Transfer **112**, 28 (2011).
[14]L. Wang, S. Kassi, A. W. Liu, S. M. Hu, and A. Campargue, J. Quant. Spectrosc. Radiat. Transfer **112**, 937 (2011).
[15]A. Campargue, L. Wang, D. Mondelain, S. Kassi, B. Bézard, E. Lellouch, A. Coustenis, C. de Bergh, M. Hirtzig, and P. Drossart, Icarus **219**, 110 (2012).
[16]A. Campargue, O. Leshchishina, L. Wang, D. Mondelain, S. Kassi, and A. V. Nikitin, J. Quant. Spectrosc. Radiat. Transfer **113**, 1855 (2012).
[17]L. Wang, D. Mondelain, S. Kassi, and A. Campargue, J. Quant. Spectrosc. Radiat. Transfer **113**, 47 (2012).
[18]A. V. Nikitin, V. Boudon, C. Wenger, S. Albert, L. R. Brown, S. Bauerecker, and M. Quack, Phys. Chem. Chem. Phys. **15**, 10071 (2013).
[19]M. Rey, A. V. Nikitin, and V. G. Tyuterev, Phys. Chem. Chem. Phys. **15**, 10049 (2013).
[20]O. N. Ulenikov, E. S. Bekhtereva, S. Albert, S. Bauerecker, H. M. Niederer, and M. Quack, J. Chem. Phys. **141**, 234302 (2014).
[21]O. Votava, M. Masat, P. Pracna, D. Mondelain, S. Kassi, A. W. Liu, S. M. Hu, and A. Campargue, J. Quant. Spectrosc. Radiat. Transfer **149**, 64 (2014).
[22]S. Beguier, S. Kassi, and A. Campargue, J. Mol. Spectrosc. **308**, 1 (2015).
[23]S. Beguier, A. W. Liu, and A. Campargue, J. Quant. Spectrosc. Radiat. Transfer **166**, 6 (2015).
[24]A. V. Nikitin, M. Rey, S. A. Tashkun, S. Kassi, D. Mondelain, A. Campargue, and V. G. Tyuterev, J. Quant. Spectrosc. Radiat. Transfer **168**, 207 (2016).
[25]M. Rey, A. V. Nikitin, A. Campargue, S. Kassi, D. Mondelain, and V. G. Tyuterev, Phys. Chem. Chem. Phys. **18**, 176 (2016).
[26]B. Amyay, M. Louviot, O. Pirali, R. Georges, J. Vander Auwera, and V. Boudon, J. Chem. Phys. **144**, 024312 (2016).
[27]R. E. Lupu, M. S. Marley, N. Lewis, M. Line, W. A. Traub, and K. Zahnle, e-print arXiv:1604.05370.
[28]A. Campargue, O. Leshchishina, L. Wang, D. Mondelain, and S. Kassi, J. Mol. Spectrosc. **291**, 16 (2013).
[29]O. L. Polyansky, A. G. Császár, S. V. Shirin, N. F. Zobov, P. Barletta, J. Tennyson, D. W. Schwenke, and P. J. Knowles, Science **299**, 539 (2003).
[30]D. W. Schwenke, Spectrochim. Acta, Part A **58**, 849 (2002).
[31]A. Yachmenev, S. N. Yurchenko, T. Ribeyre, and W. Thiel, J. Chem. Phys. **135**, 074302 (2011).
[32]P. Małyszek and J. Koput, J. Comput. Chem. **34**, 337 (2013).
[33]A. Owens, S. N. Yurchenko, A. Yachmenev, J. Tennyson, and W. Thiel, J. Chem. Phys. **142**, 244306 (2015).
[34]A. Owens, S. N. Yurchenko, A. Yachmenev, and W. Thiel, J. Chem. Phys. **143**, 244317 (2015).
[35]T. Helgaker, W. Klopper, and D. P. Tew, Mol. Phys. **106**, 2107 (2008).
[36]K. A. Peterson, D. Feller, and D. A. Dixon, Theor. Chem. Acc. **131**, 1079 (2012).
[37]T. J. Lee, J. M. L. Martin, and P. R. Taylor, J. Chem. Phys. **102**, 254 (1995).
[38]R. Marquardt and M. Quack, J. Chem. Phys. **109**, 10628 (1998).
[39]R. Marquardt and M. Quack, J. Phys. Chem. A **108**, 3166 (2004).
[40]X. G. Wang and E. L. Sibert, J. Chem. Phys. **111**, 4510 (1999).
[41]D. W. Schwenke and H. Partridge, Spectrochim. Acta, Part A **57**, 887 (2001).
[42]C. Oyanagi, K. Yagi, T. Taketsugu, and K. Hirao, J. Chem. Phys. **124**, 064311 (2006).
[43]R. Warmbier, R. Schneider, A. R. Sharma, B. J. Braams, J. M. Bowman, and P. H. Hauschildt, Astron. Astrophys. **495**, 655 (2009).
[44]A. V. Nikitin, M. Rey, and V. G. Tyuterev, Chem. Phys. Lett. **501**, 179 (2011).
[45]S. N. Yurchenko, J. Tennyson, R. J. Barber, and W. Thiel, J. Mol. Spectrosc. **291**, 69 (2013).
[46]S. N. Yurchenko and J. Tennyson, Mon. Not. R. Astron. Soc. **440**, 1649 (2014).
[47]X.-G. Wang and T. Carrington, Jr., J. Chem. Phys. **141**, 154106 (2014).
[48]M. Majumder, S. E. Hegger, R. Dawes, S. Manzhos, X.-G. Wang, T. Carrington, Jr., J. Li, and H. Guo, Mol. Phys. **113**, 1823 (2015).
[49]J. Tennyson and S. N. Yurchenko, Mon. Not. R. Astron. Soc. **425**, 21 (2012).
[50]J. Tennyson, S. N. Yurchenko, A. F. Al-Refaie, E. J. Barton, K. L. Chubb, P. A. Coles, S. Diamantopoulou, M. N. Gorman, C. Hill, A. Z. Lam, L. Lodi, L. K. McKemmish, Y. Na, A. Owens, O. L. Polyansky, T. Rivlin, C. Sousa-Silva, D. S. Underwood, A. Yachmenev, and E. Zak, J. Mol. Spectrosc. **327**, 73 (2016).
[51]J. I. Canty, P. W. Lucas, S. N. Yurchenko, J. Tennyson, S. K. Leggett, C. G. Tinney, H. R. A. Jones, B. Burningham, D. J. Pinfield, and R. L. Smart, Mon. Not. R. Astron. Soc. **450**, 454 (2015).
[52]S. N. Yurchenko, J. Tennyson, J. Bailey, M. D. J. Hollis, and G. Tinetti, Proc. Natl. Acad. Sci. U. S. A. **111**, 9379 (2014).
[53]A. Yachmenev and S. N. Yurchenko, J. Chem. Phys. **143**, 014105 (2015).
[54]S. N. Yurchenko, W. Thiel, and P. Jensen, J. Mol. Spectrosc. **245**, 126 (2007).
[55]R. I. Ovsyannikov, W. Thiel, S. N. Yurchenko, M. Carvajal, and P. Jensen, J. Chem. Phys. **129**, 044309 (2008).
[56]A. G. Császár, W. D. Allen, and H. F. Schaefer III, J. Chem. Phys. **108**, 9751 (1998).
[57]T. B. Adler, G. Knizia, and H.-J. Werner, J. Chem. Phys. **127**, 221106 (2007).
[58]K. A. Peterson, T. B. Adler, and H.-J. Werner, J. Chem. Phys. **128**, 084102 (2008).
[59]S. Ten-No, Chem. Phys. Lett. **398**, 56 (2004).
[60]J. G. Hill, K. A. Peterson, G. Knizia, and H.-J. Werner, J. Chem. Phys. **131**, 194105 (2009).
[61]K. E. Yousaf and K. A. Peterson, J. Chem. Phys. **129**, 184108 (2008).
[62]F. Weigend, Phys. Chem. Chem. Phys. **4**, 4285 (2002).
[63]C. Hättig, Phys. Chem. Chem. Phys. **7**, 59 (2005).
[64]H.-J. Werner, P. J. Knowles, G. Knizia, F. R. Manby, and M. Schütz, WIREs Comput. Mol. Sci. **2**, 242 (2012).
[65]J. G. Hill, S. Mazumder, and K. A. Peterson, J. Chem. Phys. **132**, 054108 (2010).
[66]M. Kállay and J. Gauss, J. Chem. Phys. **123**, 214105 (2005).
[67]M. Kállay and J. Gauss, J. Chem. Phys. **129**, 144101 (2008).
[68]MRCC, A string-based quantum chemical program suite written by M. Kállay; see also M. Kállay and P. R. Surján, J. Chem. Phys. **115**, 2945 (2001), as well as www.mrcc.hu.
[69]A quantum chemical program package written by J. F. Stanton, J. Gauss, M. E. Harding, and P. G. Szalay with contributions from A. A. Auer, R. J. Bartlett, U. Benedikt, C. Berger, D. E. Bernholdt, Y. J. Bomble, L. Cheng, O. Christiansen, M. Heckert, O. Heun, C. Huber, T.-C. Jagau, D. Jonsson, J. Jusélius, K. Klein, W. J. Lauderdale, D. A. Matthews, T. Metzroth, L. A. Mück, D. P. O'Neill, D. R. Price, E. Prochnow, C. Puzzarini, K. Ruud, F. Schiffmann, W. Schwalbach, S. Stopkowicz, A. Tajti, J. Vázquez, F. Wang, J. D. Watts, and the integral packages MOLECULE (J. Almlöf and P. R. Taylor), PROPS (P. R. Taylor), ABACUS (T. Helgaker, H. J. Aa. Jensen, P. Jørgensen, and J. Olsen), and ECP routines by A. V. Mitin and C. van Wüllen, for the current version, CFOUR, 2014, see http://www.cfour.de.
[70]T. H. Dunning, Jr., J. Chem. Phys. **90**, 1007 (1989).
[71]M. Douglas and N. M. Kroll, Ann. Phys. **82**, 89 (1974).
[72]B. A. Heß, Phys. Rev. A **33**, 3742 (1986).
[73]W. A. de Jong, R. J. Harrison, and D. A. Dixon, J. Chem. Phys. **114**, 48 (2001).
[74]G. Tarczay, A. G. Császár, W. Klopper, and H. M. Quiney, Mol. Phys. **99**, 1769 (2001).
[75]J. Gauss, A. Tajti, M. Kállay, J. F. Stanton, and P. G. Szalay, J. Chem. Phys. **125**, 144111 (2006).
[76]P. R. Bunker and P. Jensen, *Molecular Symmetry and Spectroscopy*, 2nd ed. (NRC Research Press, Ottawa, 1998).
[77]H. Partridge and D. W. Schwenke, J. Chem. Phys. **106**, 4618 (1997).
[78]J. K. G. Watson, J. Mol. Spectrosc. **219**, 326 (2003).
[79]T. J. Lee and P. R. Taylor, Int. J. Quantum Chem. **36**, 199 (1989).
[80]S. N. Yurchenko, R. J. Barber, A. Yachmenev, W. Thiel, P. Jensen, and J. Tennyson, J. Phys. Chem. A **113**, 11845 (2009).
[81]B. V. Noumerov, Mon. Not. R. Astron. Soc. **84**, 592 (1924).
[82]J. W. Cooley, Math. Comput. **15**, 363 (1961).
[83]G. A. Petersson, A. Bennett, T. G. Tensfeldt, M. A. Al-Laham, W. A. Shirley, and J. Mantzaris, J. Chem. Phys. **89**, 2193 (1988).
[84]G. A. Petersson and M. A. Al-Laham, J. Chem. Phys. **94**, 6081 (1991).

[85]C. Manca Tanner and M. Quack, Mol. Phys. **110**, 2111 (2012).
[86]R. Z. Martinez, D. Bermejo, J. Santos, J.-P. Champion, and J. C. Hilico, J. Chem. Phys. **107**, 4864 (1997).
[87]R. Georges, M. Herman, J. C. Hilico, and O. Robert, J. Mol. Spectrosc. **187**, 13 (1998).
[88]J. F. Stanton, Mol. Phys. **97**, 841 (1999).
[89]H. Hollenstein, R. R. Marquardt, M. Quack, and M. A. Suhm, J. Chem. Phys. **101**, 3588 (1994).
[90]C. Wenger and J. P. Champion, J. Quant. Spectrosc. Radiat. Transfer **59**, 471 (1998).
[91]M. Oldani, M. Andrist, A. Bauder, and A. G. Robiette, J. Mol. Spectrosc. **110**, 93 (1985).
[92]A. Yachmenev, I. Polyak, and W. Thiel, J. Chem. Phys. **139**, 204308 (2013).
[93]S. N. Yurchenko, R. J. Barber, J. Tennyson, W. Thiel, and P. Jensen, J. Mol. Spectrosc. **268**, 123 (2011).